 doi:10.20944/preprints202106.0226.v1

Technical Note

Global ocean studies from CALIOP/CALIPSO by removing polarization crosstalk effects

Xiaomei Lu [1,2,*], Yongxiang Hu [2,*], Ali Omar [2], Rosemary Baize [2], Mark Vaughan [2], Sharon Rodier [1,2], Jayanta Kar [1,2], Brian Getzewich [2], Patricia Lucker [1,2], Charles Trepte [2], Chris Hostetler [2], and David Winker [2]

[1] Science systems and applications, Inc. Hampton, VA, 23666, USA.
[2] NASA Langley Research Center, Hampton, VA, 23681, USA.
* Correspondence: xiaomei.lu@nasa.gov; yongxiang.hu-1@nasa.gov.

Abstract: Recent studies indicate that the Cloud-Aerosol Lidar with Orthogonal Polarization (CALIOP) aboard the Cloud-Aerosol Lidar and Infrared Pathfinder Satellite Observations (CALIPSO) satellite provides valuable information about ocean phytoplankton distributions. CALIOP's attenuated backscatter coefficients, measured at 532 nm in receiver channels oriented parallel and perpendicular to the laser's linear polarization plane, are significantly improved in the Version 4 data product. However, due to non-ideal instrument effects, a small fraction of the backscattered optical power polarized parallel to the receiver polarization reference plane is misdirected into the perpendicular channel, and vice versa. This effect, known as polarization crosstalk, typically causes the measured perpendicular signal to be higher than its true value and the measured parallel signal to be lower than its true value. Therefore, the ocean optical properties derived directly from CALIOP's measured signals will be biased if the polarization crosstalk effect is not taken into account. This paper presents methods that can be used to estimate the CALIOP crosstalk effects from on-orbit measurements. The global ocean depolarization ratios calculated both before and after removing the crosstalk effects are compared. Using CALIOP crosstalk-corrected signals is highly recommended for all ocean subsurface studies.

Keywords: CALIPSO; space lidar; ocean; depolarization ratio; crosstalk.

1. Introduction

The Cloud-Aerosol Lidar and Infrared Pathfinder Satellite Observations (CALIPSO) mission is a pioneering international partnership between NASA and the French Space Agency, CNES [1–3]. The CALIPSO mission is entering its 16th year of very successful operation, providing the first decadal dataset of high-resolution atmospheric profiles of aerosols and clouds globally [3], which are critical to earth radiation budget estimation and climate model improvements. The Cloud-Aerosol Lidar with Orthogonal Polarization (CALIOP), a dual-wavelength (532 nm and 1064 nm) polarization sensitive (at 532 nm) elastic backscatter lidar, is the prime payload instrument on the CALIPSO satellite [1]. The main objective of CALIOP is to provide global mapping of the vertical structure of the Earth's atmosphere [4].

Although CALIOP was not designed for ocean subsurface applications, its measurements over the Earth's oceans now provide a wealth of unanticipated opportunities for ocean biology and biogeochemistry studies. During the last decade, innovative retrieval methods have been developed to translate CALIOP's ocean backscattered signals into ocean optical properties such as global phytoplankton distributions [5], total particulate organic carbon (*POC*) stocks [5,6], particulate backscattering coefficients (b_{bp}, m^{-1}) [7,8], phytoplankton biomass estimates [9], and depolarization ratios of ocean waters [10,11].

However, non-ideal polarization separation by the optical components in the CALIOP receiver can cause some small fraction of the backscattered optical power polarized parallel to the receiver reference plane to be misdirected into the perpendicular channel,

Preprints (www.preprints.org) | NOT PEER-REVIEWED | Posted: 8 June 2021 doi:10.20944/preprints202106.0226.v1

and vice versa [12]. This effect, known as polarization crosstalk, typically causes the measured cross-polarized (i.e., the perpendicular channel, s) attenuated backscatter coefficient (β'_s, $m^{-1}sr^{-1}$) to be higher than its true value and the measured co-polarized (i.e., the parallel channel, p) attenuated backscatter coefficient (β'_p, $m^{-1}sr^{-1}$) to be lower than its true value [13,14].

Because the backscatter signals from beneath the ocean surface are highly attenuated, the relative errors in the CALIOP measured cross-polarized attenuated backscatter coefficient ($\frac{\beta'_{s,measured}-\beta'_{s,true}}{\beta'_{s,true}} \times 100\%$) due to crosstalk can be up to 100% or more for some scenes, which will in turn introduce biases into the subsequently derived ocean optical properties, such as b_{bp}, *POC* stocks, phytoplankton biomass, etc. Consequently, estimates of ocean optical properties derived from CALIOP measurements must take crosstalk into account and the crosstalk artifacts should be removed before retrieving ocean optical properties. Unfortunately, previous analyses of CALIOP data for ocean studies [5,7,10,11,15] did not take into account the effect of optical crosstalk between the 532 nm parallel and perpendicular channels.

The objectives of this study are to (1) estimate the magnitude of CALIOP's polarization crosstalk from on-orbit measurements, (2) provide a correction method to remove crosstalk effects on CALIOP measured attenuated backscatter coefficients, and (3) compare the ocean results retrieved before and after applying the crosstalk correction. In section 2 we describe the methods used to estimate the crosstalk from CALIOP Level 1 (L1) data and develop a straightforward correction function. The global ocean depolarization ratio results before and after crosstalk correction are compared in section 3. We conclude with a summary of our investigations in section 4.

2. Methods

The analysis and results presented in this work use CALIOP Version 4.1 (V4) Level 1 (L1) data products [16], in which the calibration of the 532 nm attenuated backscatter coefficients is significantly improved [17,18].

The CALIOP backscatter signal at 532 nm is separated into parallel (p) and perpendicular (s) components by polarization beam splitters (PBS) in the receiver subsystem [1,2]. The crosstalk (CT_{p2s}) represents the fraction of the optical power polarized parallel to the receiver polarization reference plane that is transferred to the perpendicular channel, as follows:

$$\beta'_{s,measured}(z) = \beta'_{s,true}(z) + CT_{p2s} \times \beta'_{p,true}(z) \text{ and} \quad (1)$$

$$\beta'_{p,measured}(z) = \beta'_{p,true}(z) - CT_{p2s} \times \beta'_{p,true}(z). \quad (2)$$

Here, a fraction (CT_{p2s}) of $\beta'_{p,true}$ is reflected into the perpendicular channel (Eq. 1) and that the remainder ($1-CT_{p2s}$) of the parallel signal $\beta'_{p,true}$ is transmitted into the parallel detector (Eq. 2). The polarization crosstalk from perpendicular channel to parallel channel (CT_{s2p}) is ignored in Eqs. (1) and (2) because the contribution of $CT_{s2p} \times \beta'_{s,true}(z)$ to both 532 nm channels is less than 1%, while the contribution of $CT_{p2s} \times \beta'_{p,true}(z)$ to perpendicular channel (Eq. 1) can be as large as 100% or more (section 2.3) and should be taken into account.

2.1. Crosstalk estimation from clear air depolarization ratio (method 1)

CALIOP clear air depolarization ratio measurements have no particular scientific interest, since the depolarization ratio of clear air is known to be around 0.0035 for the optical filter passbands implemented in the CALIOP receiver. However, they are of interest from an instrument performance standpoint because they allow us to monitor the crosstalk between the parallel and perpendicular channels. For this investigation, the CALIOP measured clear air depolarization ratio (δ_{mol}) is calculated as,

 doi:10.20944/preprints202106.0226.v1

$$\delta_{mol} = \sum_{z=20km}^{z=30km} \beta'_{s,measured}(z) \Big/ \sum_{z=20km}^{z=30km} \beta'_{p,measured}(z) \quad (3)$$

i.e., the mean perpendicular attenuated backscatter coefficient divided by the mean parallel attenuated backscatter coefficient, with the means computed over the altitude region from 20 km to 30 km. The signals in this altitude regime consist almost entirely of molecular backscatter. Aerosol scattering is generally negligible, and cloud contributions at these altitudes can be neglected entirely. This calculation excludes the wintertime polar regions, where polar stratospheric clouds may contribute significantly to the signal.

With an ideal beam splitter, δ_{mol} estimates obtained by using Eq. (3) would approximately equal the theoretical value of 0.0035. Absent shot noise and with perfect calibration, these δ_{mol} values would exactly equal the theoretical value. The difference between the measured and theoretical molecular depolarization ratios can indicate the level of crosstalk between the two polarization channels. From CALIOP L1 data which are well calibrated [17,18], the CT_{p2s} can be estimated as (method 1):

$$CT_{p2s} = \delta_{mol} - 0.0035, \quad (4)$$

where the measured molecular depolarization ratio (δ_{mol}) is calculated by Eq. (3) from L1 nighttime data for two chosen latitude regions: 0° to 40°N and 0° to 40°S, where the South Atlantic Anomaly (SAA) region was excluded because CALIOP is experiencing an elevated frequency of low energy laser shots due to decreased pressure inside the laser canister (https://www-calipso.larc.nasa.gov/resources/calipso_users_guide/advisory/advisory_2018-06-12.php). We choose the CALIOP nighttime measurements to avoid the effects of solar background noises on the clear air depolarization ratios.

From Eq. (4), the uncertainties of CT_{p2s} can be estimated as $(\frac{\Delta CT_{p2s}}{CT_{p2s}})^2 = (\frac{\Delta\delta_{mol}}{\delta_{mol}})^2$, where the uncertainties of δ_{mol}, $(\frac{\Delta\delta_{mol}}{\delta_{mol}})^2$ depend on the random error and possibility of bias error in polarization gain ratio (PGR). The random error is dominated by the noise in the lidar data itself. With sufficient averaging, such as averaging in 20 km – 30 km vertically, 0° - 40°N regionally and monthly (e.g., Figure 1), we will insure that the random error is low and can be neglected [12]. PGR accounts for differences in the responsivity and gain of the CALIOP's two polarization channels at 532 nm and the relative transmission of the optics downstream of the PBS [4]. The bias error in the PGR is due primarily to non-ideal polarization effects in the transmitter and receiver, e.g., non-ideal performance of the pseudo-depolarizer, the bias error of which is less than 0.26% [12].

Figure 1 shows the time series of crosstalk values calculated from CALIOP L1 data (monthly) by Eq. (4) from June 2006 to November 2020 (green and black). The monthly crosstalk values over two chosen regions 0°-40°N and 0°-40°S (without SAA) are shown in green and black in Figure 1. The dashed blue line in Figure 1 indicates when CALIOP was switched from the primary laser to the backup laser, i.e., Feb. 2009. The most likely explanation for the discrete jumps in April 2009 and February 2020 over the latitude region from 0° to 40°S (black line in Figure 1) is depolarizing smoke injected into the stratosphere by Australia bushfires [19,20]. No corresponding changes are seen in either the PGR or the crosstalk estimated over the northern hemisphere (0°-40°N. green in Figure 1) in those months. Similarly, the northern hemisphere crosstalk jumps seen in September and October 2017 are mainly due to pyrocumulonimbus (pyroCb) smoke events in western North America in August 2017 [21]. In contrast to the tropospheric smoke, the stratospheric smoke resulting from pyroCb events have significant depolarization [22], which impacts the crosstalk calculation. Excluding these explainable excursions, the relative differences of crosstalk values between the two chosen regions are less than 10%, with the root mean square of differences about 0.03%.

Preprints (www.preprints.org) | NOT PEER-REVIEWED | Posted: 8 June 2021 doi:10.20944/preprints202106.0226.v1

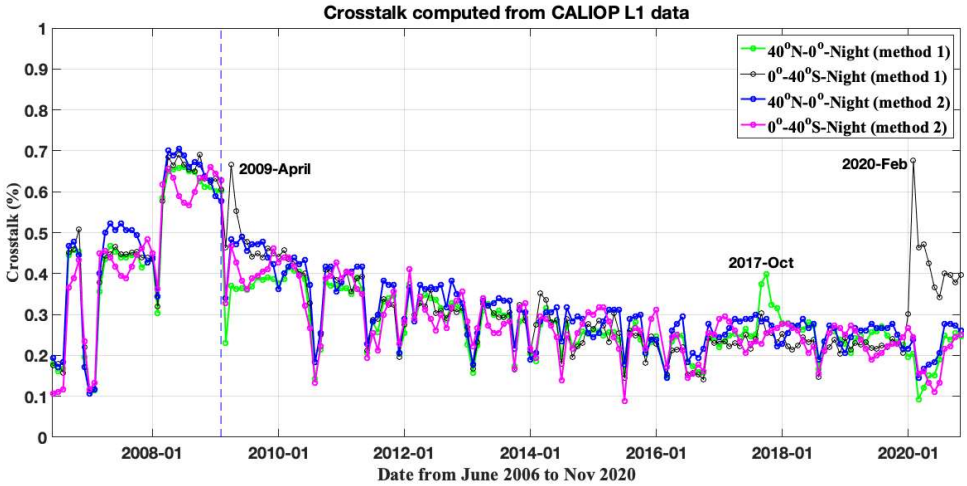

Figure 1. Time series of crosstalk calculated from CALIOP L1 data by method 1 and 2 from June 2006 to November 2020 over two chosen regions 0°-40°N (green by method 1 and blue by method 2) and 0°-40°S (black by method 1 and pink by method 2). The dashed blue line indicates when CALIOP was switched from the primary laser to the backup laser (i.e., Feb. 2009). The discrete jumps in April 2009, September/October 2017, and February 2020 by method 1 are most likely due to the depolarizing smoke injected into the stratosphere. See details in text.

2.2. Crosstalk estimation from ocean surface return (method 2)

Under this method, we use the CALIOP L1 532 nm signals from the range bin that includes the ocean surface reflection. In doing so, we take into account that the vertical resolution of this bin is 30 m (in air, 23 m in water), and therefore includes signal contributions from the atmosphere and the ocean subsurface in addition to the laser surface reflection. In both 532-nm channels, the atmospheric contribution is much smaller than the ocean surface and subsurface reflection and can be neglected. For a linearly polarized incident lidar beam (e.g., CALIOP), spherical particles, molecular (Rayleigh) scattering and the laser reflection at the ocean surface do not contribute significantly to cross polarization [11]. As a result, cross-polarized signal measured by the perpendicular channel is dominated by the backscatter from non-spherical particles, e.g., plankton and other non-spherical particles and multiple scattering from all particles, while the co-polarized signal measured by the parallel channel is overwhelmingly from the ocean surface reflection [5], which depends on the wind speed [23]. Thus, the correlation between the true parallel ($\beta'_{p,true}$) and perpendicular ($\beta'_{s,true}$) signals backscattered from ocean should be a minimum.

Our second method to estimate the crosstalk takes advantage of this lack of correlation between the scattering in the two 532 nm polarization channels. The measured ocean layer-integrated attenuated backscatter (unit: sr^{-1}) in two polarization channels are defined as:

$$\gamma_{s,measured} = \int_{z(p_i-1)}^{z(p_i+3)} \beta'_{s,measured}(z)dz, \quad (5)$$

$$\gamma_{p,measured} = \int_{z(p_i-1)}^{z(p_i+3)} \beta'_{p,measured}(z)dz. \quad (6)$$

where we are integrating over 5 range bins and p_i indicates the altitude index of the peak ocean surface return bin. The ocean surface lidar backscatter (Eqs. 5 and 6) is a integrating of the measured attenuated backscatter coefficients from 1 bin above to 3 bins below the peak bin because of CALIOP's low pass filter and detector transient response [23]. Here, x=($\gamma_{s,measured} - CT_{p2s} \times \gamma_{p,measured}$) represents the corrected cross-polarized signal with

Preprints (www.preprints.org) | NOT PEER-REVIEWED | Posted: 8 June 2021 doi:10.20944/preprints202106.0226.v1

the CT_{p2s} changing from 0 to 2%, and y=$\gamma_{p,measured}$ is the co-polarized signal depending on wind speed. The absolute value of correlation coefficient (ρ_{xy}) is used as a performance function:

$$\rho_{xy} = |corr(x,\ y)|, \tag{7}$$

where "| |" in Eq. (7) refer to absolute value. A series of trial values of the CT_{p2s} between 0 to 2% with an increment of 0.01% is used to calculate the correlation coefficients (ρ_{xy}) in Eq. (7). Finally, the crosstalk is determined by searching a minimum value of the performance function of Eq. (7) (method 2). Compared with Eq. 4, the second method does not require the measured clean air depolarization ratio δ_{mol} or the theoretical value of clear air depolarization ratio of 0.0035 used in Eq. 4. It uses the measured ocean layer-integrated attenuated backscatter at the two polarization channels (Eqs, 5, 6 and 7) to estimate the crosstalk.

The time series of crosstalk values calculated from level 1 ocean backscattered signals by method 2 from June 2006 to November 2020 over two chosen regions: 0 to 40°N and 0 to 40°S are shown as blue and pink in Figure 1. The monthly crosstalk values estimated from level 1 ocean backscattered signals (method 2) during nighttime are compared with those estimated by method 1 (green and black in Figure 1). The relative differences of crosstalk values retrieved by method 1 and method 2 are less than 10%, with the root mean square of differences ~0.04%. Figure 2 shows the crosstalk differences between night and day ($CT_{p2s,night} - CT_{p2s,day}$) over two chosen regions 0°-40°N (red) and 0°-40°S (dark blue). The mean difference of crosstalk between day and night shown in Figure 2 is less than 5%, with the root mean square of differences about 0.03%.

One of the key goals in the design of CALIOP was to achieve less than 1% crosstalk. Figures 1 and 2 clearly show that the polarization crosstalk is less than 1%, which indicates the excellent performance of CALIOP.

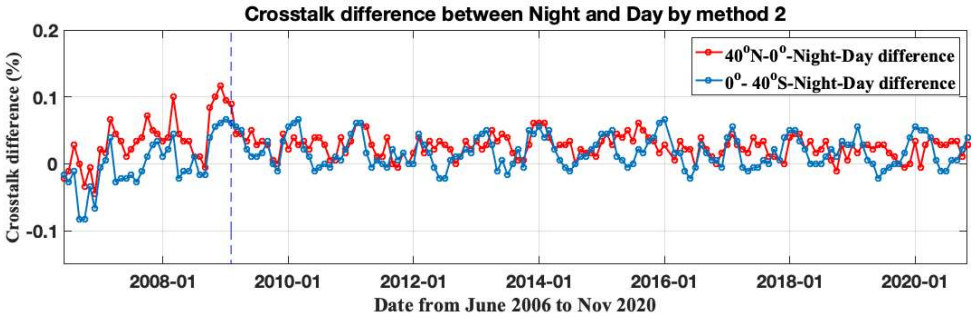

Figure 2. Time series of crosstalk difference between night and day ($CT_{p2s,night} - CT_{p2s,day}$) calculated from CALIOP L1 ocean signals by method 2 from June 2006 to November 2020 over two chosen regions 0°-40°N (red) and 0°-40°S (dark blue). The dashed blue line indicates when CALIOP was switched from the primary laser to the backup laser (i.e., Feb. 2009).

2.3. Effects of Crosstalk on measured ocean backscattered signals

Even though the crosstalk values are less than 1% over the entire CALIOP mission (Figures 1 and 2), its effects on perpendicular channel ocean signals can still be large [13]. We illustrate this with a heuristic example that assumes the true ocean backscattered signals are $\beta'_{s,true}$=1 km^{-1} sr^{-1} and $\beta'_{p,true}$ = 100 km^{-1} sr^{-1}, yielding a depolarization ratio of 1% (e.g., as in Figures 3-6). Given a polarization crosstalk of 0.5% (e.g., Figure 2), the measured ocean signals given by Eq. 1 and 2 will be $\beta'_{s,measured}$ = 1.5 km^{-1} sr^{-1} and $\beta'_{p,measured}$=99.5 km^{-1} sr^{-1}, with a corresponding measured depolarization ratio slightly above 1.5%. The relative error ($\frac{\beta'_{s,measured}-\beta'_{s,true}}{\beta'_{s,true}} \times 100\%$) of the measured perpendicular signal and depolarization ratio are ~50%. The impact of crosstalk increases as the true depolarization ratio decreases and exerts its largest effects in oceanic regions where

Preprints (www.preprints.org) | NOT PEER-REVIEWED | Posted: 8 June 2021 doi:10.20944/preprints202106.0226.v1

concentrations of phytoplankton are especially low and hence the true ocean depolarization ratio approaches its minimum. As seen in figures 5 and 6, the depolarization ratios seen over extensive swaths of the ocean are significantly less than 1%, leading to large crosstalk-induced errors (e.g., Figure 8) and highlighting the motivation for correcting the data before using the L1 backscatter signals for ocean subsurface retrievals.

From Eqs. (1) and (2), the crosstalk-corrected attenuated backscatter coefficients ($\beta'_{p,correct}, \beta'_{s,correct}$) can be derived from the measured signals as:

$$\beta'_{p,correct}(z) = \beta'_{p,measured}(z)/(1 - CT_{p2s}), \text{ and} \quad (8)$$

$$\beta'_{s,correct}(z) = \beta'_{s,measured}(z) - CT_{p2s} \times \beta_{p,correct}(z). \quad (9)$$

Using CALIOP crosstalk-corrected signals (Eqs. 8 and 9) is highly recommended for all ocean subsurface studies.

3. Global ocean results

This section compares the global ocean depolarization ratios after crosstalk correction with those before crosstalk correction. The integrated cross- (γ_s, sr^{-1}) and co-polarization (γ_p, sr^{-1}) components of the total ocean subsurface backscatters are obtained from CALIOP crosstalk-corrected ocean attenuated backscatter coefficients $\beta'_{p,correct}(z)$ and $\beta'_{s,correct}(z)$ as:

$$\gamma_s = \int_{z(p_i-1)}^{z(p_i+3)} \beta'_{s,correct}(z)dz, \quad (10)$$

$$\gamma_p = \int_{z(p_i-1)}^{z(p_i+3)} \beta'_{p,correct}(z)dz. \quad (11)$$

where p_i indicates the altitude index of the peak ocean surface return bin. The total depolarization ratio of ocean water, which includes contributions from water molecules and in-water particulate matter, is defined as:

$$\delta_t = \frac{\gamma_s}{\gamma_p} \quad (12)$$

The seasonal distributions in CALIOP's total ocean depolarization ratio before crosstalk correction (ratio between Eq. 5 and 6) during both nighttime and daytime are shown in Figures 3 and 4, respectively. Data are seasonally averaged climatologies for the 2008-2020 period and binned to 1° latitude × 1° longitude pixels. For comparison, the seasonal distributions of crosstalk corrected total depolarization ratios using Eq. (12) are given in Figures 5 and 6 for nighttime and daytime, respectively.

The ocean depolarization ratios before crosstalk correction shown in Figures 3 and 4 are substantially larger than the depolarization ratios after crosstalk correction (Figures 5 and 6). From Figures 3 and 4, the depolarization ratio is ~1% over most of the permanently stratified oceans: i.e., the low nutrient and low biomass waters, between roughly 40°N and 40°S, excluding coastal regions and the Eastern Pacific upwelling regions. However, the crosstalk corrected depolarization ratio (Figures 5 and 6) is ~0.4% over most of these same regions.

Figure 7 presents the histograms of depolarization ratios before (orange) and after (sky blue) crosstalk correction. These results indicate that the mean relative differences in the depolarization ratios before and after crosstalk correction ($\frac{\delta_{t,before}-\delta_{t,after}}{\delta_{t,after}} \times 100\%$) are ~55% during nighttime and ~42% during daytime. Figure 8 gives the global map of relative differences between the depolarization ratios before and after crosstalk correction ($\frac{\delta_{t,before}-\delta_{t,after}}{\delta_{t,after}} \times 100\%$) during daytime, which indicate over the low nutrient, low

Preprints (www.preprints.org) | NOT PEER-REVIEWED | Posted: 8 June 2021 doi:10.20944/preprints202106.0226.v1

biomass waters between roughly 40°N and 40°S, the crosstalk-induced errors in the depolarization ratios before crosstalk correction are very high and can be as large as 200%. As a result, using CALIOP crosstalk-corrected signals is highly recommended for all ocean subsurface studies.

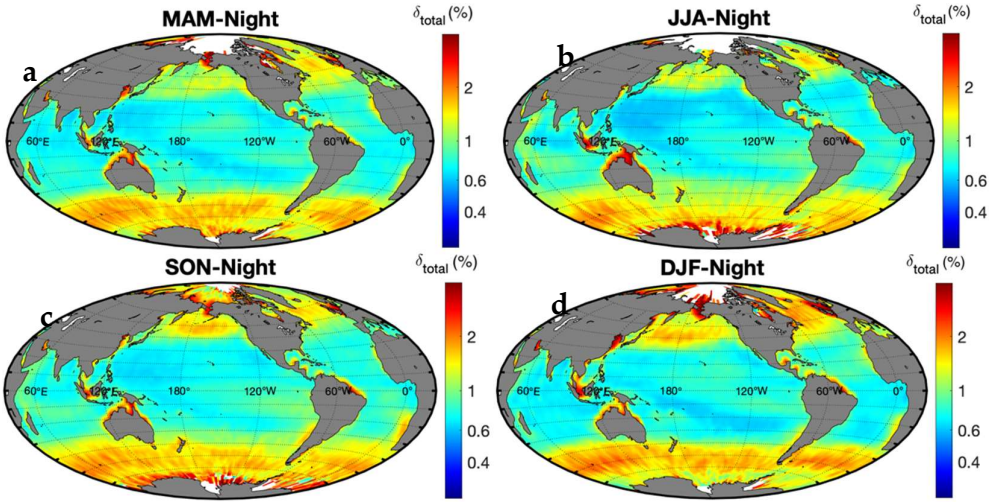

Figure 3. Seasonal distributions of CALIOP total depolarization ratio (δ_t, %) at nighttime before crosstalk correction. (a) March - May; (b) June - August; (c) September - November; (d) December - February. Data are seasonal average climatology for the 2006-2020 period and have been averaged to 1° latitude × 1° longitude pixels.

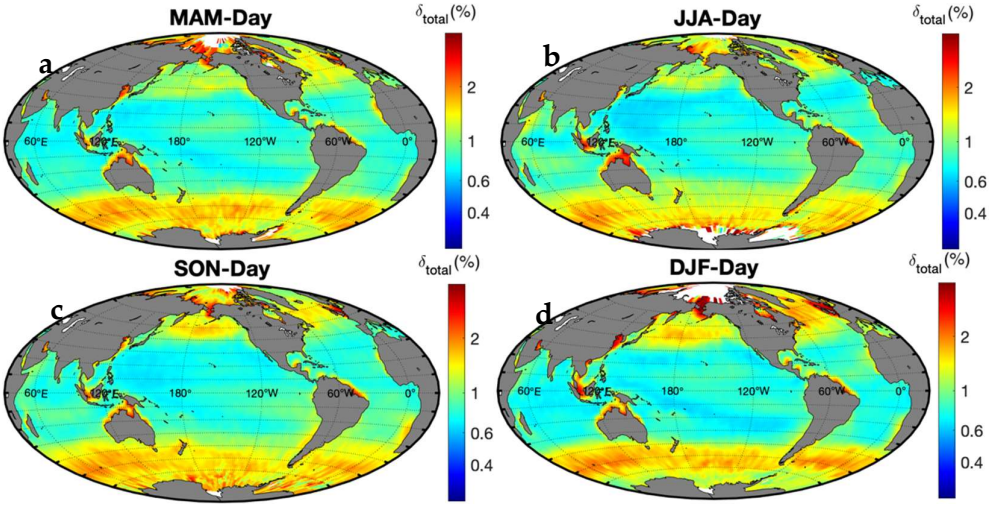

Figure 4. Same with Fig. 3 but for daytime results before crosstalk correction.

Preprints (www.preprints.org) | NOT PEER-REVIEWED | Posted: 8 June 2021 doi:10.20944/preprints202106.0226.v1

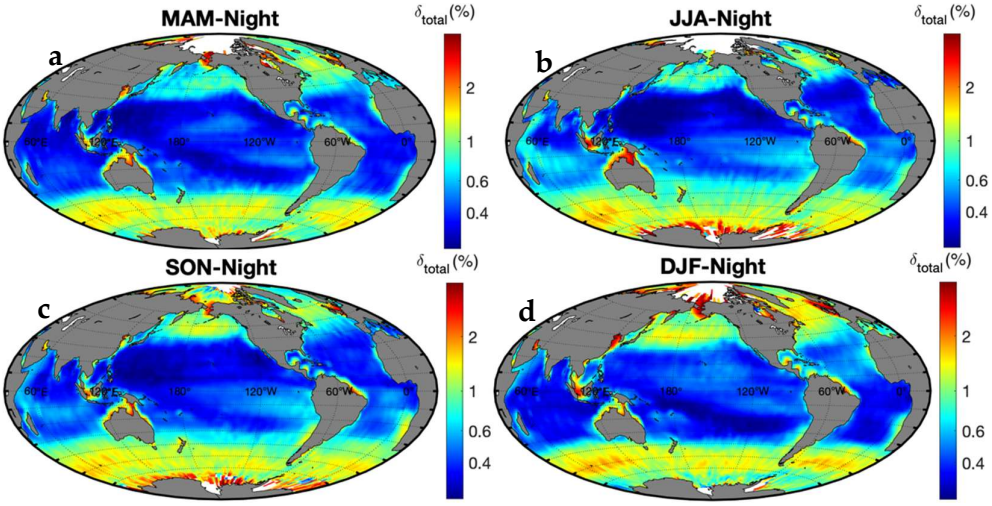

Figure 5. Seasonal distributions of CALIOP total depolarization ratio (δ_t, %) at nighttime after crosstalk correction. (a) March - May; (b) June - August; (c) September - November; (d) December - February. Data are seasonal average climatology for the 2008-2020 period and have been averaged to 1° latitude × 1° longitude pixels.

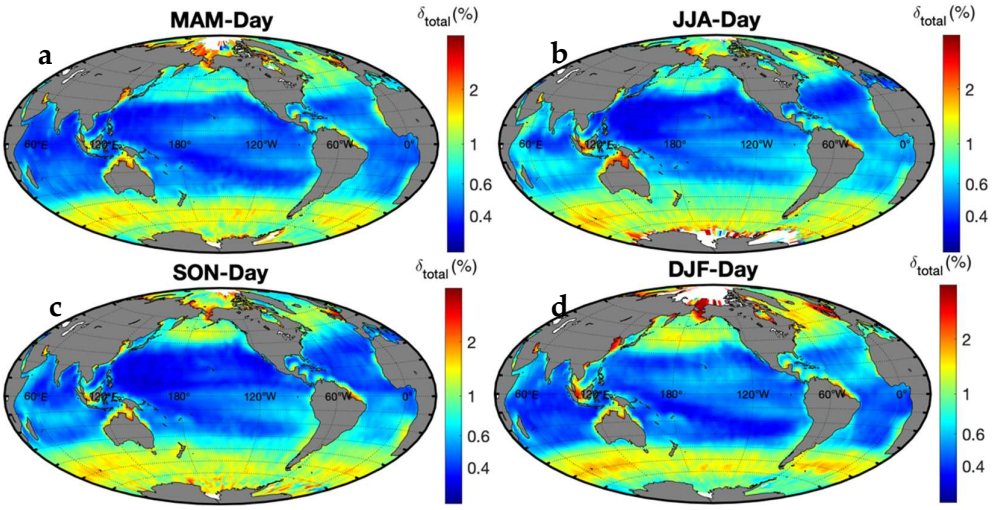

Figure 6. Same with Fig. 5 but for daytime results after crosstalk correction.

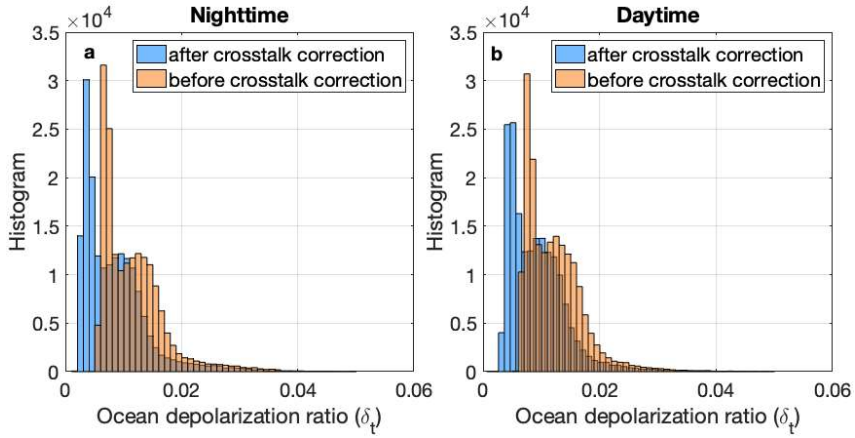

Figure 7. Ocean total depolarization ratio comparisons after (sky blue color) and before (orange color) crosstalk corrections during (a) nighttime and (b) daytime.

Preprints (www.preprints.org) | NOT PEER-REVIEWED | Posted: 8 June 2021 doi:10.20944/preprints202106.0226.v1

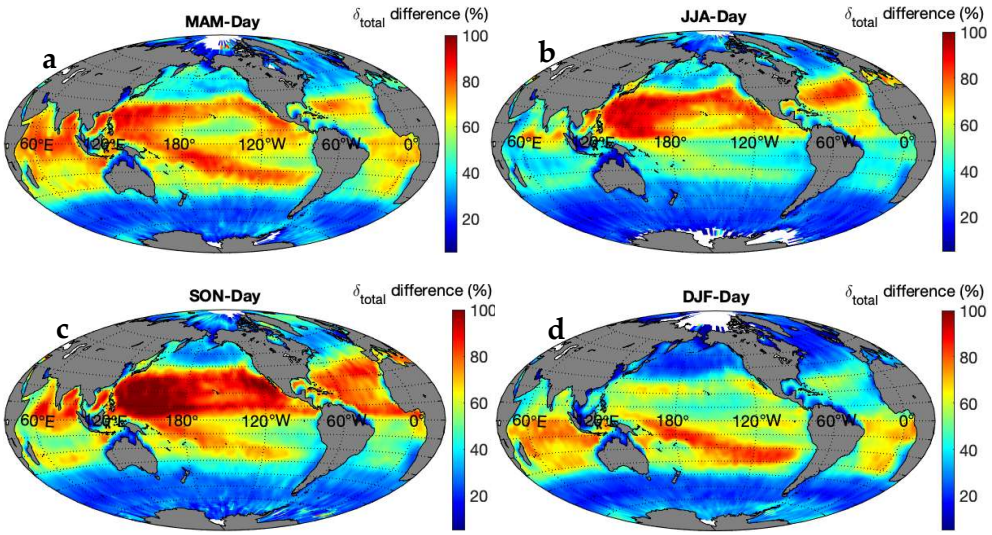

Figure 8. Relative differences between the depolarization ratios before and after crosstalk correction ($\frac{\delta_{t,before}-\delta_{t,after}}{\delta_{t,after}} \times 100\%$) at daytime. (a) March - May; (b) June - August; (c) September - November; (d) December - February.

4. Discussion and Conclusions

In this study, we introduce two approaches to estimate the polarization crosstalk between CALIOP's 532 nm parallel and perpendicular channels. Both estimates are obtained directly from the CALIOP Level 1 data. Crosstalk magnitudes can be estimated from the clear air depolarization ratios measured between 20 and 30 km (methods 1) and from the ocean backscattered signals in the parallel and perpendicular channels (method 2). The advantage of the second method is that it does not require use of the measured clean air depolarization ratio (which can be contaminated by intermittent injections of stratospheric aerosols), nor does it require explicit knowledge of either the polarization gain ratio or the theoretical value of the clear air depolarization ratio. The CALIOP crosstalk values retrieved by both methods are less than 1% over the CALIPSO entire mission, thus verifying that the engineering design goal of less than 1% crosstalk between the two polarization channels at 532 nm has been successfully accomplished and setting the standard for future space-based lidar missions.

The proposed crosstalk correction methods have been used to correct CALIOP's measurements of attenuated backscatter coefficients at the near surface of the Earth's oceans. The global ocean total depolarization ratios are retrieved from the corrected ocean attenuated backscatter coefficients and are compared with those before crosstalk correction. The results indicate the relative errors of ocean total depolarization ratio before crosstalk correction are ~55% during nighttime and ~42% during daytime and can be up to 200% over low-nutrient and low-biomass oceans. As a result, using CALIOP crosstalk-corrected signals is highly recommended for all ocean subsurface studies e.g., calculations of b_{bp}, *POC*, phytoplankton biomass, etc. Our results strongly support the continued use of CALIOP measurements to study the global plankton system of the upper ocean.

Author Contributions: Conceptualization, X. Lu. and Y.Hu.; methodology, Y.Hu. and X.Lu.; formal analysis, X. Lu. and Y.Hu.; investigation, X. Lu., Y.Hu., M. Vaughan., S. Rodier, and B. Getzewich; resources, C. Trepte., D. Winker, M. Vaughan., A.Omar., B. Getzewich; writing—original draft preparation, X. Lu.; writing—review and editing, all authors; supervision, A. Omar, R. Baize and P.Lucker.; project administration, C. Trepte and P.Lucker.; funding acquisition, X. Lu. All authors have read and agreed to the published version of the manuscript.

Funding: This research was funded by NASA awards, grant numbers 80NSSC20K0129 and 80NSSC21K0910.

Data Availability Statement: The authors would like to thank the NASA CALIPSO data acquisition and analysis teams for providing the data used in this study. The CALIPSO V4.10 lidar level 1 data used in this study is publicly available and can be freely accessed via https://doi.org/10.5067/CALIOP/CALIPSO/LID_L1-Standard-V4-10.

Conflicts of Interest: The authors declare no conflict of interest.

References

1. Hunt, W.H.; Winker, D.M.; Vaughan, M.A.; Powell, K.A.; Lucker, P.L.; Weimer, C. CALIPSO Lidar Description and Performance Assessment. *Journal of Atmospheric and Oceanic Technology* **2009**, *26*, 1214–1228, doi:10.1175/2009JTECHA1223.1.
2. Winker, D.M.; Vaughan, M.A.; Omar, A.; Hu, Y.; Powell, K.A.; Liu, Z.; Hunt, W.H.; Young, S.A. Overview of the CALIPSO Mission and CALIOP Data Processing Algorithms. *Journal of Atmospheric and Oceanic Technology* **2009**, *26*, 2310–2323, doi:10.1175/2009jtecha1281.1.
3. Winker, D.M.; Pelon, J.; Coakley, J.A.; Ackerman, S.A.; Charlson, R.J.; Colarco, P.R.; Flamant, P.; Fu, Q.; Hoff, R.M.; Kittaka, C.; et al. The CALIPSO Mission: A Global 3D View of Aerosols and Clouds. *Bulletin of the American Meteorological Society* **2010**, *91*, 1211–1229, doi:10.1175/2010bams3009.1.
4. Powell, K.A.; Hostetler, C.A.; Vaughan, M.A.; Lee, K.-P.; Trepte, C.R.; Rogers, R.R.; Winker, D.M.; Liu, Z.; Kuehn, R.E.; Hunt, W.H.; et al. CALIPSO Lidar Calibration Algorithms. Part I: Nighttime 532-Nm Parallel Channel and 532-Nm Perpendicular Channel. *Journal of Atmospheric and Oceanic Technology* **2009**, *26*, 2015–2033, doi:10.1175/2009jtecha1242.1.
5. Behrenfeld, M.J.; Hu, Y.; Hostetler, C.A.; Dall'Olmo, G.; Rodier, S.D.; Hair, J.W.; Trepte, C.R. Space-Based Lidar Measurements of Global Ocean Carbon Stocks. *Geophysical Research Letters* **2013**, *40*, 4355–4360, doi:10.1002/grl.50816.
6. Lu, X.; Hu, Y. Estimation of Particulate Organic Carbon in the Ocean from Space-Based Polarization Lidar Measurements.; 2014; Vol. 9261, pp. 92610Z-92610Z–8.
7. Lacour, L.; Larouche, R.; Babin, M. In Situ Evaluation of Spaceborne CALIOP Lidar Measurements of the Upper-Ocean Particle Backscattering Coefficient. *Opt. Express* **2020**, *28*, 26989–26999, doi:10.1364/OE.397126.
8. Lu, X.; Hu, Y.; Pelon, J.; Trepte, C.; Liu, K.; Rodier, S.; Zeng, S.; Lucker, P.; Verhappen, R.; Wilson, J.; et al. Retrieval of Ocean Subsurface Particulate Backscattering Coefficient from Space-Borne CALIOP Lidar Measurements. *Opt. Express* **2016**, *24*, 29001–29008, doi:10.1364/OE.24.029001.
9. Behrenfeld, M.J.; Hu, Y.; O'Malley, R.T.; Boss, E.S.; Hostetler, C.A.; Siegel, D.A.; Sarmiento, J.L.; Schulien, J.; Hair, J.W.; Lu, X.; et al. Annual Boom-Bust Cycles of Polar Phytoplankton Biomass Revealed by Space-Based Lidar. *Nature Geosci* **2017**, *10*, 118–122, doi:10.1038/ngeo2861.
10. Dionisi, D.; Brando, V.E.; Volpe, G.; Colella, S.; Santoleri, R. Seasonal Distributions of Ocean Particulate Optical Properties from Spaceborne Lidar Measurements in Mediterranean and Black Sea. *Remote Sensing of Environment* **2020**, *247*, 111889, doi:10.1016/j.rse.2020.111889.
11. Lu, X.; Hu, Y.; Trepte, C.; Zeng, S.; Churnside, J.H. Ocean Subsurface Studies with the CALIPSO Spaceborne Lidar. *Journal of Geophysical Research: Oceans* **2014**, *119*, 4305–4317, doi:10.1002/2014jc009970.
12. Chris A. Hostetler; Liu, Z.; Reagan, J.; Vaughan, M.; Winker, D.; Osborn, M.; Hunt, W.; Powell, K.; Trepte, C. CALIOP Algorithm Theoretical Basis Document Calibration and Level 1 Data Products. *PC-SCI-201 Release 1.0* **2006**, doi:https://www-calipso.larc.nasa.gov/resources/pdfs/PC-SCI-201v1.0.pdf.
13. Lu, X.; Hu, Y.; Yang, Y.; Neumann, T.A.; Omar, A.; Baize, R.; Vaughan, M.; Rodier, S.; Getzewich, B.; Trepte, C.; et al. New Ocean Subsurface Optical Properties from Space Lidars: CALIOP/CALIPSO and ATLAS/ICESat-2. *Earth and Space Science* **2021**, *submitted-under review*, doi:https://doi.org/10.1002/essoar.10507064.1.
14. Pitts, M.C.; Poole, L.R.; Gonzalez, R. Polar Stratospheric Cloud Climatology Based on CALIPSO Spaceborne Lidar Measurements from 2006 to 2017. *Atmospheric Chemistry and Physics* **2018**, *18*, 10881–10913, doi:10.5194/acp-18-10881-2018.

15. Bisson, K.M.; Boss, E.; Werdell, P.J.; Ibrahim, A.; Behrenfeld, M.J. Particulate Backscattering in the Global Ocean: A Comparison of Independent Assessments. *Geophysical Research Letters* **2021**, *48*, e2020GL090909, doi:10.1029/2020GL090909.
16. Vaughan, M.; Pitts, M.; Trepte, C.; Winker, D.; Detweiler, P.; Garnier, A.; Getzewich, B.; Hunt, W.; Lambeth, J.; Lee, K.-P.; et al. Cloud – Aerosol LIDAR Infrared Pathfinder Satellite Observations (CALIPSO) Data Management System Data Products Catalog. **2020**, *Document No: PC-SCI-503*, doi:https://www-calipso.larc.nasa.gov/products/CALIPSO_DPC_Rev4x92.pdf.
17. Kar, J.; Vaughan, M.A.; Lee, K.-P.; Tackett, J.L.; Avery, M.A.; Garnier, A.; Getzewich, B.J.; Hunt, W.H.; Josset, D.; Liu, Z.; et al. CALIPSO Lidar Calibration at 532 Nm: Version 4 Nighttime Algorithm. *Atmos. Meas. Tech.* **2018**, *11*, 1459–1479, doi:10.5194/amt-11-1459-2018.
18. Getzewich, B.J.; Vaughan, M.A.; Hunt, W.H.; Avery, M.A.; Powell, K.A.; Tackett, J.L.; Winker, D.M.; Kar, J.; Lee, K.-P.; Toth, T.D. CALIPSO Lidar Calibration at 532 Nm: Version 4 Daytime Algorithm. *Atmos. Meas. Tech.* **2018**, *11*, 6309–6326, doi:10.5194/amt-11-6309-2018.
19. Siddaway, J.M.; Petelina, S.V. Transport and Evolution of the 2009 Australian Black Saturday Bushfire Smoke in the Lower Stratosphere Observed by OSIRIS on Odin. *Journal of Geophysical Research: Atmospheres* **2011**, *116*, doi:10.1029/2010JD015162.
20. Khaykin, S.; Legras, B.; Bucci, S.; Sellitto, P.; Isaksen, L.; Tencé, F.; Bekki, S.; Bourassa, A.; Rieger, L.; Zawada, D.; et al. The 2019/20 Australian Wildfires Generated a Persistent Smoke-Charged Vortex Rising up to 35 Km Altitude. *Communications Earth & Environment* **2020**, *1*, 22, doi:10.1038/s43247-020-00022-5.
21. Peterson, D.A.; Campbell, J.R.; Hyer, E.J.; Fromm, M.D.; Kablick, G.P.; Cossuth, J.H.; DeLand, M.T. Wildfire-Driven Thunderstorms Cause a Volcano-like Stratospheric Injection of Smoke. *npj Climate and Atmospheric Science* **2018**, *1*, 30, doi:10.1038/s41612-018-0039-3.
22. Christian, K.; Yorks, J.; Das, S. Differences in the Evolution of Pyrocumulonimbus and Volcanic Stratospheric Plumes as Observed by CATS and CALIOP Space-Based Lidars. *Atmosphere* **2020**, *11*, doi:10.3390/atmos11101035.
23. Hu, Y.; Stamnes, K.; Vaughan, M.; Pelon, J.; Weimer, C.; Wu, D.; Cisewski, M.; Sun, W.; Yang, P.; Lin, B.; et al. Sea Surface Wind Speed Estimation from Space-Based Lidar Measurements. *Atmos. Chem. Phys.* **2008**, *8*, 3593–3601, doi:10.5194/acp-8-3593-2008.